MASTER

EXPERIMENTAL TEST OF RESONANT ABSORPTION THEORY

Final Report
for Period January 1, 1978 - December 31, 1979

Eli Yablonovitch

Harvard University
Cambridge, Massachusetts 02138

NOTICE

May 1979

Prepared For

THE U. S. DEPARTMENT OF ENERGY
UNDER CONTRACT NO. AS02-78DP 40018
(Old Contract No. ED-78-S-02-4631)

DISCLAIMER

EXPERIMENTAL TEST OF RESONANT ABSORPTION THEORY

Abstract

This experimental research has probed the nature of resonant absorption (RA) of laser light by laser-produced plasmas. The plasmas were created by optical breakdown of a shockfront produced in an electrothermal shock tube. This procedure allows the density structure of the plasma, and in particular, the orientation of the plasma critical-density surface, to be reproducibly formed from one shot to the next. Thus, for the first time, RA has been controllably and reproducibly studied in isolation from other plasma physics. The angular distribution of fast electrons emitted by RA and "wavebreaking" has been studied, and it is observed that the emission is directed in a narrow cone centered on the shockfront density-gradient vector, in agreement with the theory of wavebreaking. This unidirectional emission allows the construction of a simple magnetic-focussing electron spectrometer, which yields the "temperature", T_h, of the suprathermal tail of the electron energy spectrum. For 500 psec FWHM laser pulses with $I\lambda^2 \sim 10^{16}$ W-$\mu m^2/cm^2$, it is found that T_h scales with laser intensity I as $T_h \propto I^{\delta}$, where $\delta = .32 \pm .03$. This is in agreement with predictions of the theory of profile modification by the ponderomotive force. For much shorter laser pulses (20 psec risetime, 100 to 200 psec FWHM), the scaling exponent δ is found to be $\delta = .1 \pm .1$, in disagreement with theory. This observation seems to be due to the dominance of a transient regime in which most electrons are emitted in a "chirped" monoenergetic pulse of 1 to 2 psec duration. In this model the observed electron energy spectrum is due to the integrated temporal variation of the energy of the electron burst. A numerical calculation of this effect yields the same scalings as seen experimentally.

Introduction

Resonant Absorption (RA) is an important mechanism of laser-plasma interaction. This polarization and angle-of-incidence dependent mechanism can account for the substantial absorption of laser light by plasmas that has been seen experimentally during the last decade. Unfortunately, in a real laser-plasma interaction experiment, the target tends to deform and disassemble hydrodynamically in a time comparable to the laser pulse duration. Thus the plasma geometry and density structure, which are so important in RA, is rarely well known or reproducible. This often makes interpretation in terms of RA indirect at best and impossible at worst. The goal of this research has been to overcome this problem by creating a reproducible, well-characterized target. In this way experimental data can be directly related to the properties of the target. Extraneous effects, such as hydrodynamics, turbulence, and stimulated scattering, do not seem to play a role and are ignored.

Apparatus

The target is created by optical breakdown of a shockfront produced in an electrothermal shock tube, as shown in Figure 1. The shock tube discharge drives a shock of strength $M \approx 5$ in D_2 gas at a pressure in the range 35-70 Torr. Just behind such a shockfront in 43 Torr D_2, the neutral density of deuterium atoms is exactly the critical density, $n_{cr} = 10^{19}$ cm^{-3}, for a CO_2 laser light. Breakdown of the shockfront by a short, intense CO_2 laser pulse ($I \sim 10^{14}$ W/cm^2, 100-500 psec FWHM) thus produces a plasma whose density rises from subcritical, ahead of the shock, to critical behind it. The structure and orientation of this plasma density gradient are reproducibly controlled by the shock tube.

As shown in Figure 1, the detection of the moving shockfront, and its synchronization with the laser pulse, are performed by a two-channel laser Schlieren system. The two He-Ne laser beams are deflected past the Schlieren knife edges and into the photodiode as the shockfront passes them, producing two signal pulses which are used to trigger the main CO_2 laser pulse. The position of the shockfront at the time of arrival of the main laser pulse can be determined to within a few focal depths of the final focussing lens.

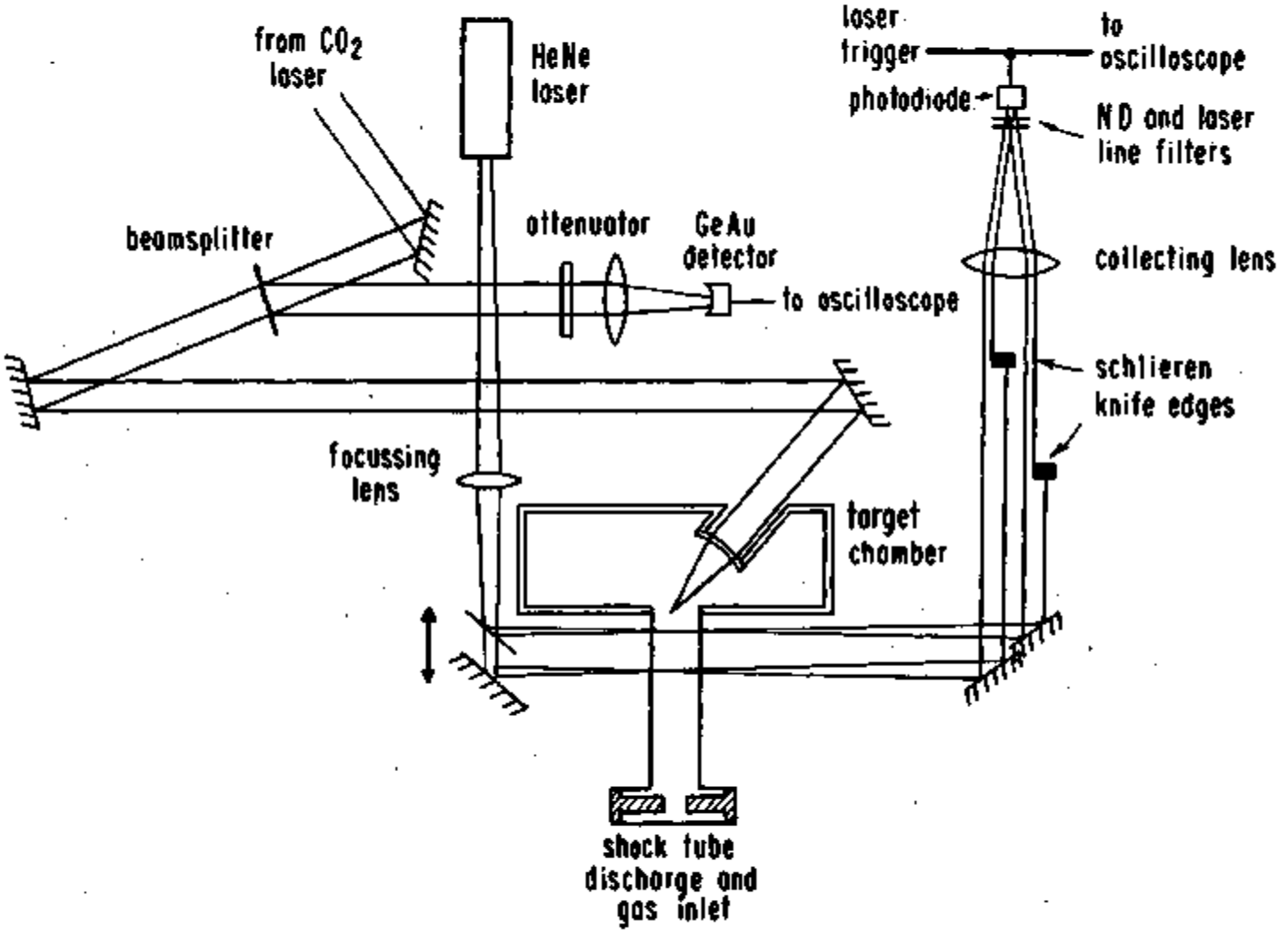

Figure 1. Layout of the experimental apparatus, showing the laser-schlieren shockfront detection system.

With a properly synchronized shockfront target, a 500 psec FWHM laser pulse, focussed to $I \sim 10^{14}$ W/cm^2 with an f/1 lens, causes electron emission from the plasma. The electronic signal, caused by detecting this emission with a Si surface-barrier detector, is plotted as a function of shockfront position in Figure 2. The large enhancement obtained when the shockfront is in proper focus demonstrates the beneficial effect of the presence of the shockfront in the laser focus.

This electron emission has been recorded on X-ray film wrapped in Al foil. The emission from a properly focussed shockfront is seen to lie in a narrow cone centered on the shocktube axis. Emission along the plasma density-gradient vector, as seen in this experiment, is characteristic of the wave-breaking mechanism. In addition, the electron emission from homogeneous gaseous targets in the same apparatus displays the angular and polarization dependences characteristic of RA.

The unidirectional nature of the electron emission just described has allowed the construction of a magnetic-focussing electron spectrometer. For this purpose, the target chamber, which holds the final focussing lens in proper relation to the shock tube, was placed between the poles of a small permanent magnet. Thus the electron trajectories, initially directed along the shock tube axis, are now focussed in a plane perpendicular to that axis, as shown in Figure 3. In the focal plane is placed an array of charge collectors whose signals thus determine an electron energy spectrum. A typical spectrum is shown in Figure 4. The dark bars along the horizontal axis denote the energy widths of the charge collectors. A standard two-temperature spectrum is obtained, with a suprathermal "tail" whose "temperature", T_h, was 36 keV in this shot. An important series of experiments consists of studying T_h as a function of external parameters, as will now be described.

Results

Experimental values of T_h obtained with 500 psec FWHM laser pulses in D_2 shockfront targets, are plotted in Figure 5 as a function of laser pulse energy. A least-squares fit of the form $T_h \propto E_p^{\delta}$ yields a scaling exponent $\delta = .32 \pm .03$. This scaling law is consistent with the well-known model of self-consistent profile modification by the ponderomotive force, which pre-

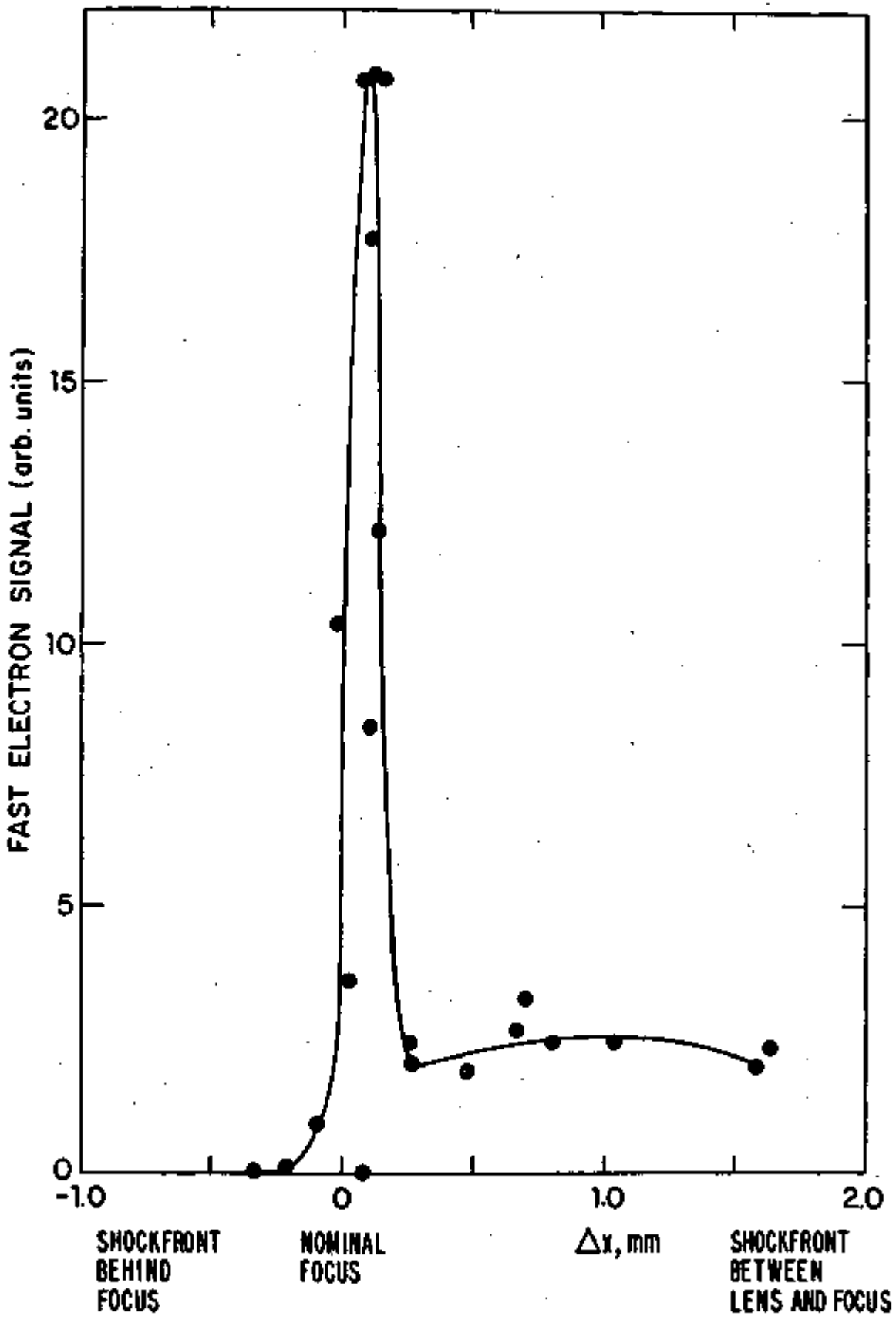

Figure 2. Electron signal vs. shockfront position for a shockfront with M = 5 in 43 Torr D_2.

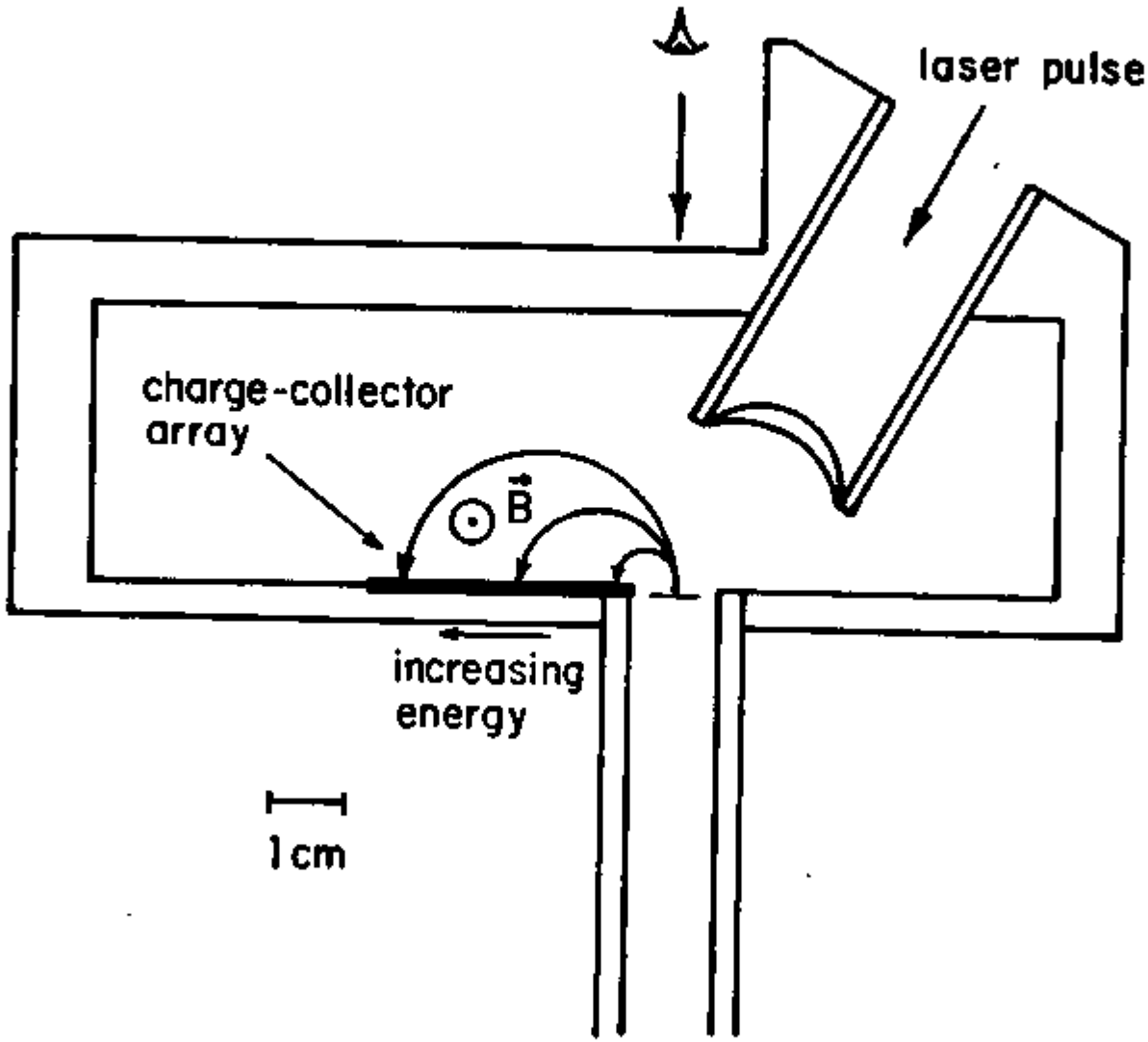

Figure 3. Sketch of magnetic-focussing electron spectrometer.

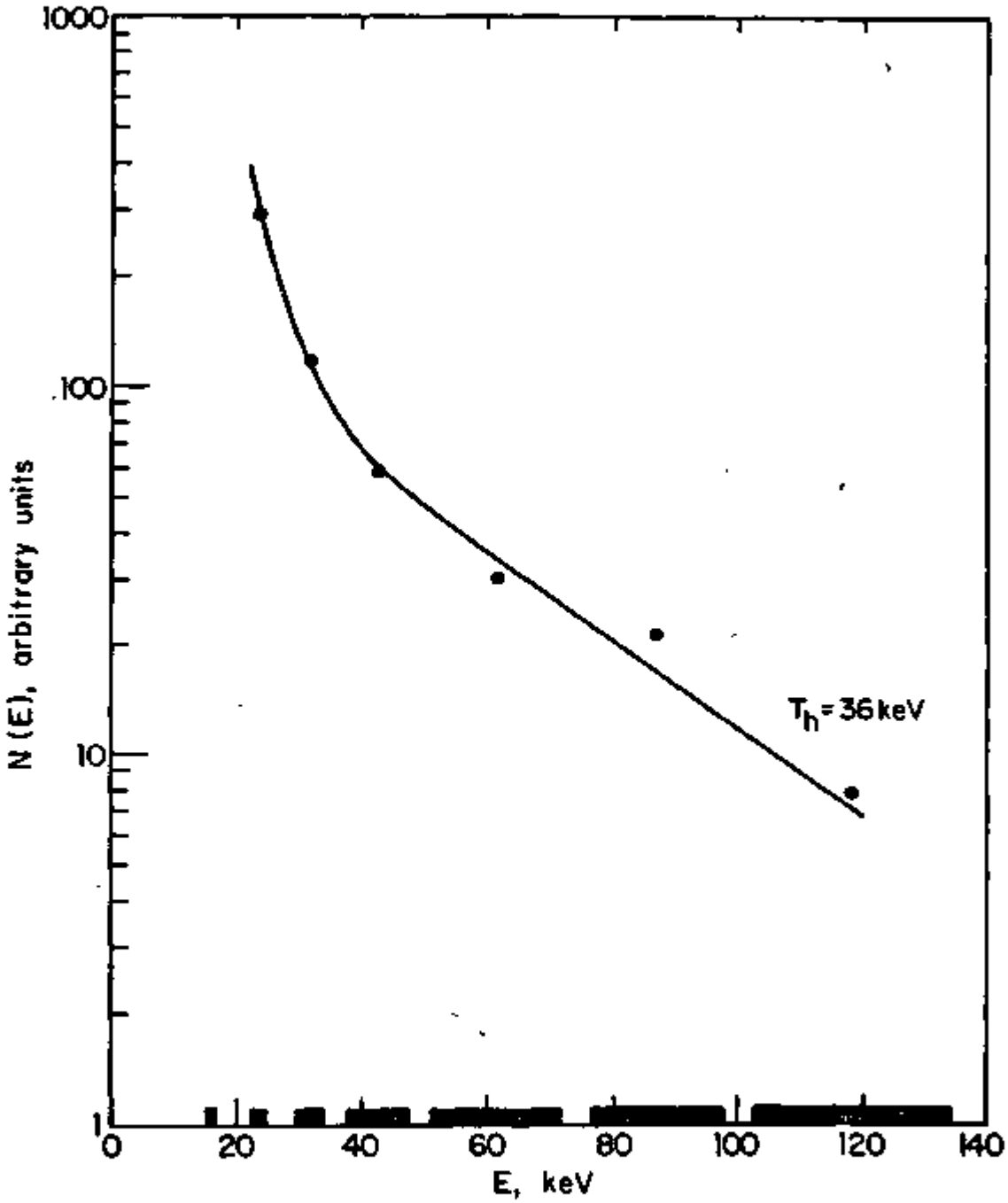

Figure 4. A typical electron energy spectrum.

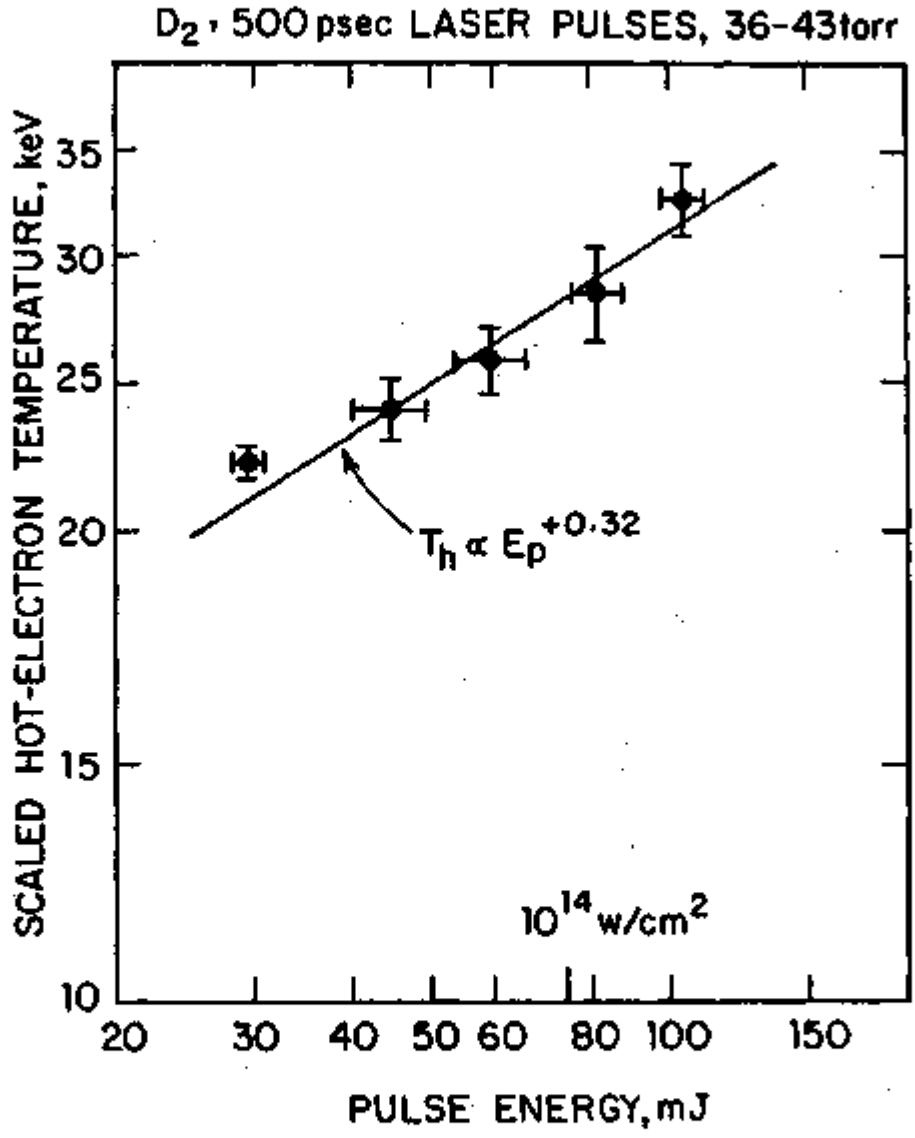

Figure 5. Hot electron temperature vs. laser pulse energy in D_2 for 500 psec FWHM laser pulses.

dicts $\delta = .32 - .39$. The threshold for profile modification is exceeded early in the laser pulse, and the interaction time is sufficiently long to allow complete profile steepening as seen in computer simulations. This model is therefore applicable to the present experiment.

This is not the case for experiments using fast risetime (20 psec) laser pulses. The identity of experimental results (Figures 6, 7 and 8) obtained with 20 psec risetime laser pulses of varying durations (100 to 200 psec FWHM) implies that the interaction is over before the peak of the pulse (this is consistent with computer calculations described below). Thus there is not enough time for profile modification to occur, and this model does not predict the experimentally observed scaling exponent $\delta = .1 \pm .1$ (see Figures 6 and 7). However, the experimental scalings with both pressure and laser pulse energy are correctly predicted by a numerical calculation which postulates that electron emission at each instant in time is mono-energetic, with an energy determined by RA and wavebreaking in the plasma density profile at that time. The plasma density profile is due to avalanche ionization of the shockfront. An important result of this calculation is that, once ionization has proceeded enough to produce a critical density (typically 5-7 psec after the start of the laser pulse), electron emission is a very rapid process. Electrons of energies detected in this experiment are emitted in a burst of 1 to 2 psec duration, and the electron energy changes dramatically even over this short time, as seen in Figure 9. Thus the experimental spectrum is just the integrated temporal variation of the electron energy, and the scaling of the resulting suprathermal tail temperature T_h with laser energy and pressure is shown in Figure 10. The calculated temperatures are slightly lower than observed experimentally, but the scaling with laser energy and pressure matches experimental observations quite well.

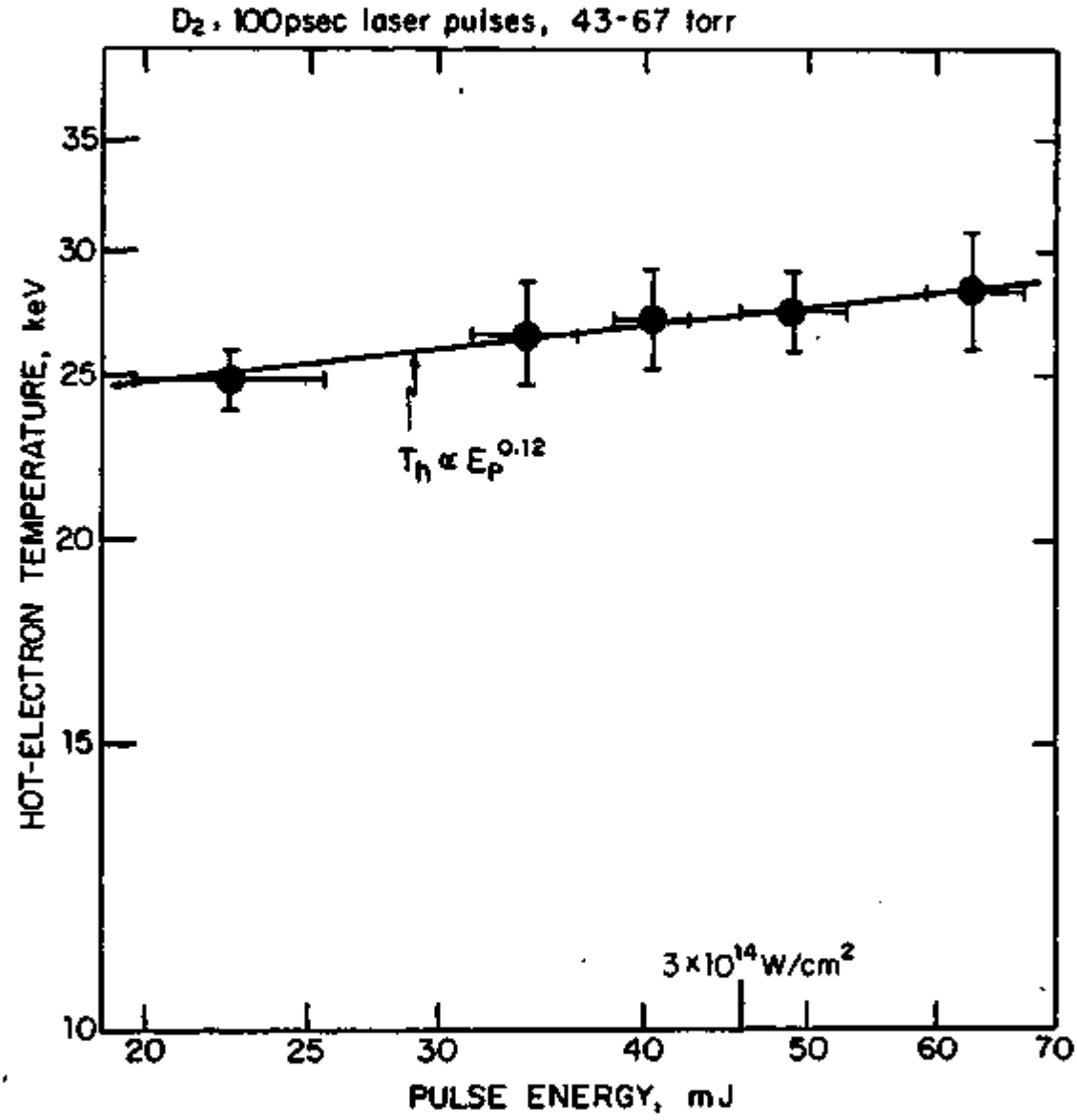

Figure 6. Hot electron temperature vs. laser pulse energy in D_2 for 100 psec FWHM laser pulses.

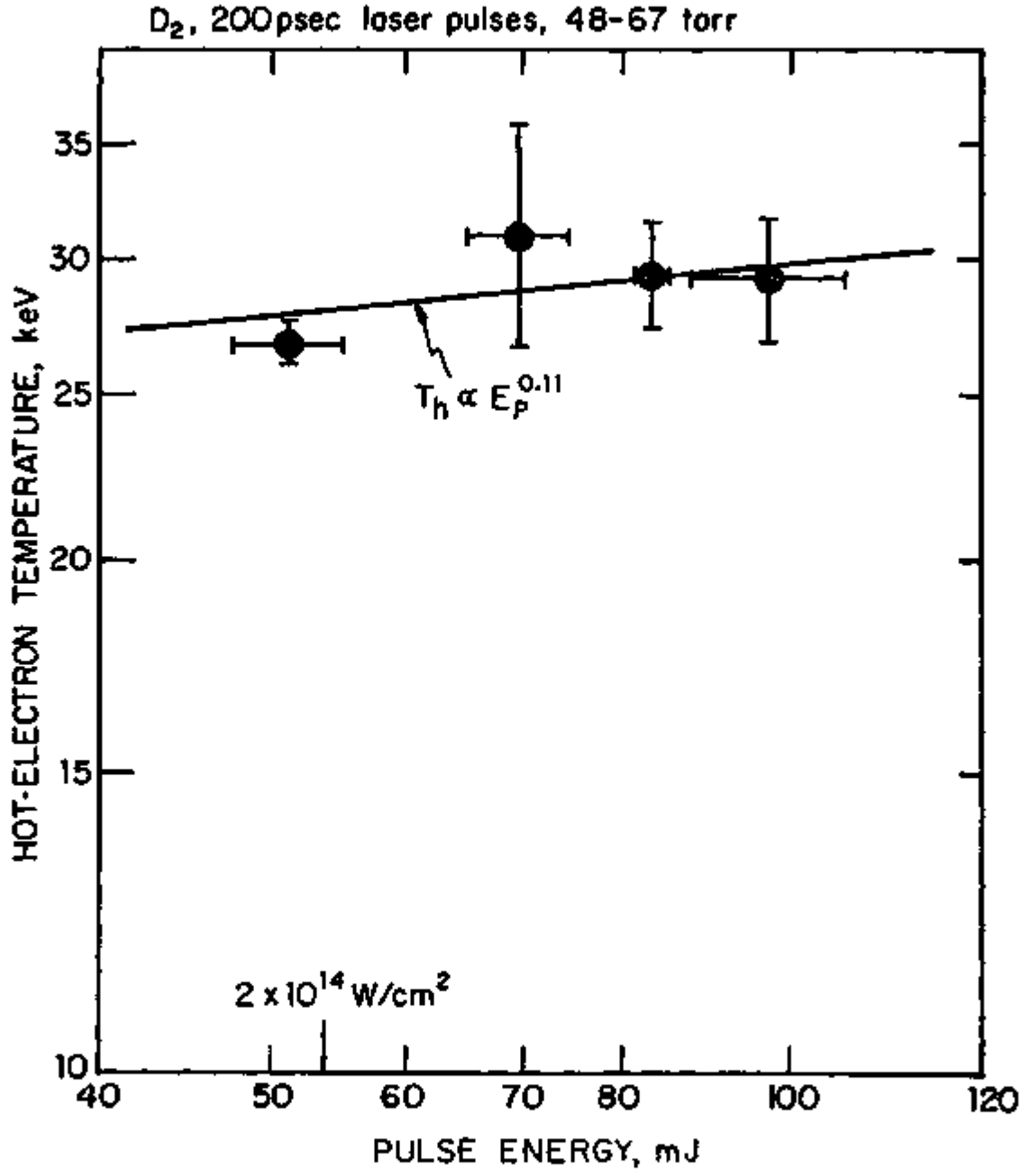

Figure 7. Hot electron temperature vs. laser pulse energy in D_2 for 200 psec FWHM laser pulses.

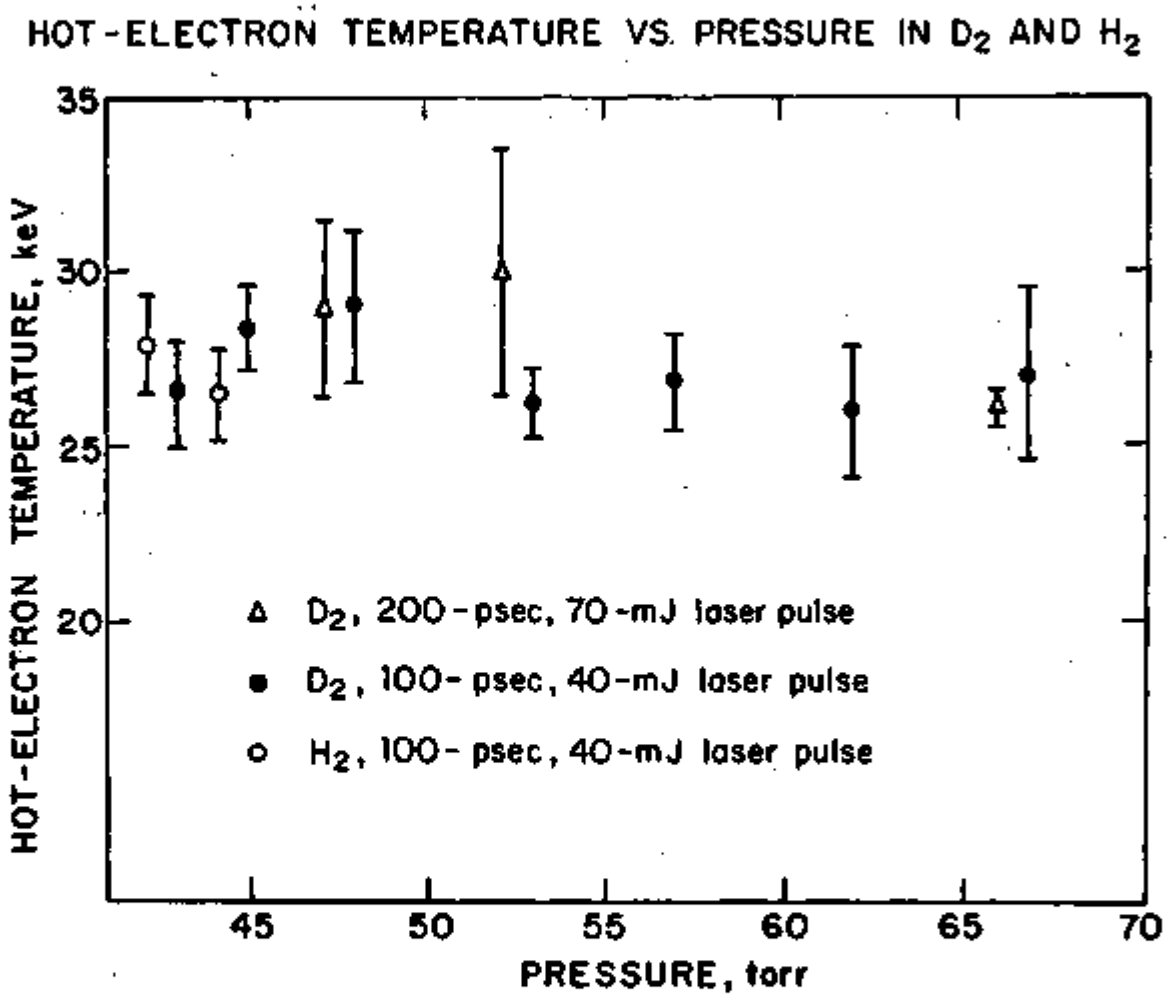

Figure 8. Hot electron temperature vs. pressure in D_2 and H_2 for 100 psec and 200 psec FWHM laser pulses.

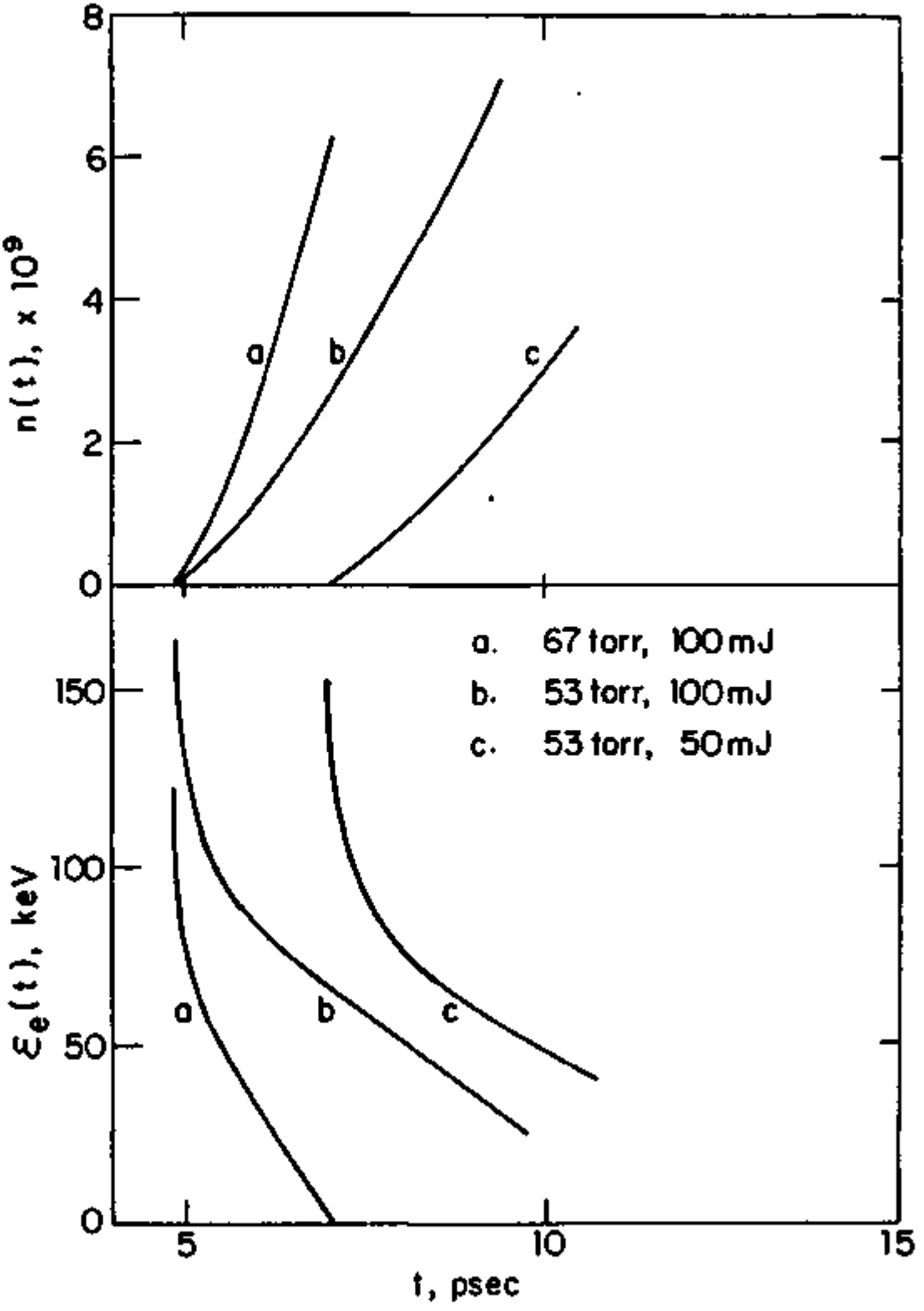

Figure 9. Energy (bottom) and integrated number (top) of electrons emitted from various shockfronts as a function of time after the start of irradiation by a 20 psec risetime laser pulse.

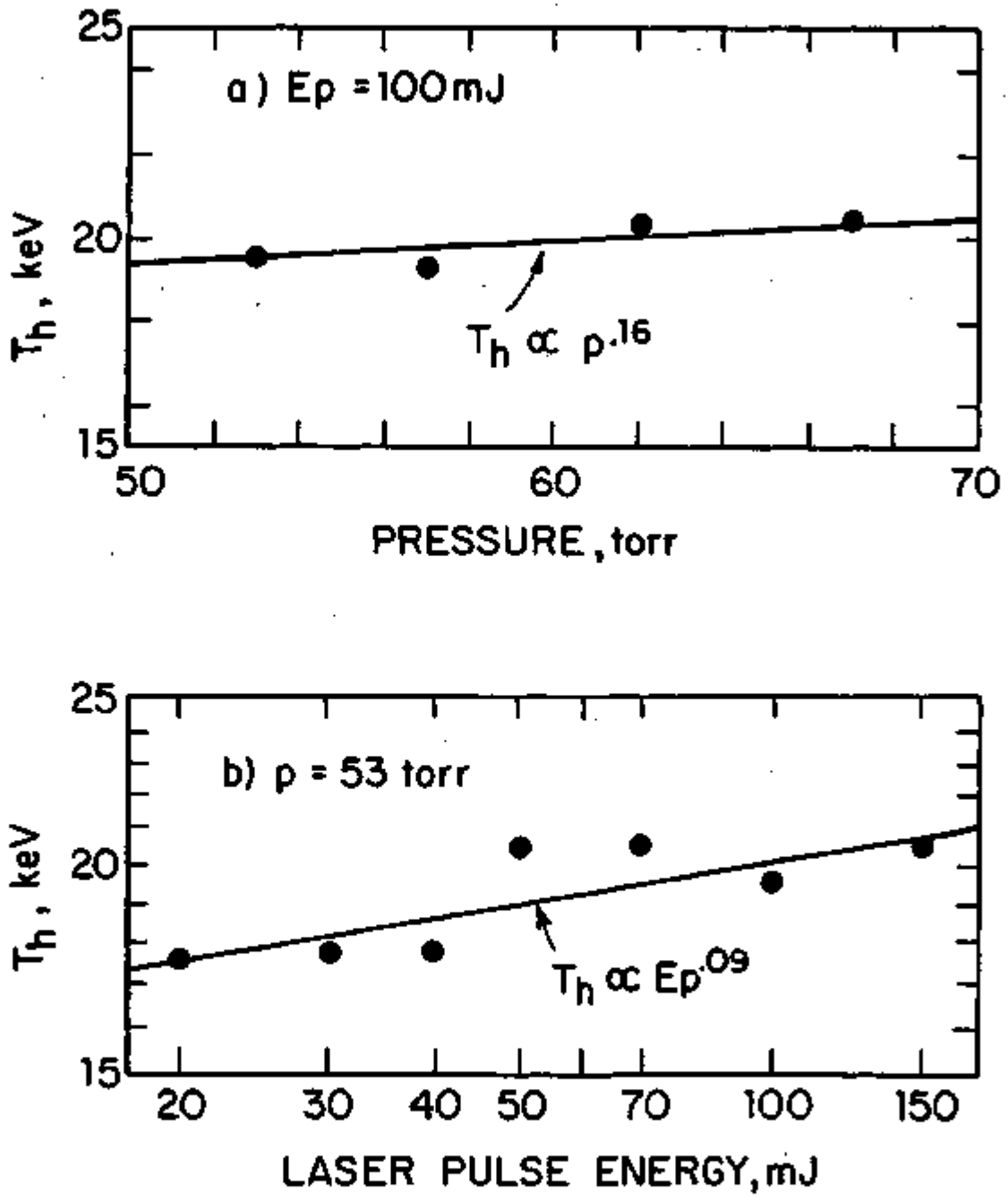

Figure 10. Calculated scaling of hot electron temperature with pressure and laser pulse energy.